Andrew R. Laich
Center for Advanced Turbomachinery and Energy Research,
Mechanical and Aerospace Engineering,
University of Central Florida,
Orlando, FL 32816
e-mail: alaich@knights.ucf.edu

Jessica Baker
Center for Advanced Turbomachinery and Energy Research,
Mechanical and Aerospace Engineering,
University of Central Florida,
Orlando, FL 32816
e-mail: jessicablueb@Knights.ucf.edu

Erik Ninnemann
Center for Advanced Turbomachinery and Energy Research,
Mechanical and Aerospace Engineering,
University of Central Florida,
Orlando, FL 32816
e-mail: erik.ninnemann@knights.ucf.edu

Clayton Sigler
Center for Advanced Turbomachinery and Energy Research,
Mechanical and Aerospace Engineering,
University of Central Florida,
Orlando, FL 32816
e-mail: Claytonsigler4@Knights.ucf.edu

Clemens Naumann
Deutsches Zentrum für Luft- und Raumfahrt (DLR),
Institut für Verbrennungstechnik,
Stuttgart 70569, Germany
e-mail: clemens.naumann@dlr.de

Marina Braun-Unkhoff
Deutsches Zentrum für Luft- und Raumfahrt (DLR),
Institut für Verbrennungstechnik,
Stuttgart 70569, Germany
e-mail: Marina.Braun-Unkhoff@dlr.de

Subith S. Vasu[1]
Center for Advanced Turbomachinery and Energy Research,
Mechanical and Aerospace Engineering,
University of Central Florida,
Orlando, FL 32816
e-mail: subith@ucf.edu

Effects of High Fuel Loading and CO_2 Dilution on Oxy-Methane Ignition Inside a Shock Tube at High Pressure

Ignition delay times were measured for methane/O_2 mixtures in a high dilution environment of either CO_2 or N_2 using a shock tube facility. Experiments were performed between 1044 K and 1356 K at pressures near 16 ± 2 atm. Test mixtures had an equivalence ratio of 1.0 with 16.67% CH_4, 33.33% O_2, and 50% diluent. Ignition delay times were measured using OH emission and pressure time-histories. Data were compared to the predictions of two literature kinetic mechanisms (ARAMCO MECH 2.0 and GRI Mech 3.0). Most experiments showed inhomogeneous (mild) ignition which was deduced from five time-of-arrival pressure transducers placed along the driven section of the shock tube. Further analysis included determination of blast wave velocities and locations away from the end wall of initial detonations. Blast velocities were 60–80% of CJ-Detonation calculations. A narrow high temperature region within the range was identified as showing homogenous (strong) ignition which showed generally good agreement with model predictions. Model comparisons with mild ignition cases should not be used to further refine kinetic mechanisms, though at these conditions, insight was gained into various ignition behavior. To the best of our knowledge, we present first shock tube data during ignition of high fuel loading CH_4/O_2 mixtures diluted with CO_2 and N_2.* [DOI: 10.1115/1.4047023]

Keywords: shock tube, mild ignition, strong ignition, detonation, air emissions from fossil fuel combustion, alternative energy sources, energy conversion/systems, fuel combustion

Introduction

With the development of gas turbines moving toward a more efficient and cleaner future, use of methane (CH_4) combustion is being closely examined due to the negative impacts of high carbon monoxide (CO), carbon dioxide (CO_2), and nitrous oxide (NO_x) emissions and issues regarding high fuel consumption. In addition, the future of space is rapidly moving toward creating space-faring colonies and having a fuel (liquid methane) that can be easily manufactured as well as a fuel that does not require a large amount of consumption for a given power output is essential. Methane is a prime candidate rocket fuel due to its potential accessibility and manufacturability on distant worlds, such as leveraging the predominantly CO_2 atmosphere of Mars in a Sabatier reaction to yield methane [1]. Additional specific impulse improvements can be realized over more traditional methods and fuels such as liquid hydrogen and

[1]Corresponding author.

Contributed by the Advanced Energy Systems Division of ASME for publication in the Journal of Energy Resources Technology. Manuscript received April 13, 2020; final manuscript received April 13, 2020; published online May 26, 2020. Editor: Hameed Metghalchi.

kerosene (RP-1), particularly in the so-called full-flow staged combustion cycle. Typically, air and methane have been used in gas turbine engines to fuel high energy processes; however, in the presence of air, nitrous oxides and CO_2 will inevitably form exhausting into the atmosphere. By combusting methane with pure oxygen (oxy-methane) in a closed-loop CO_2 cycle, NO_x formation and exhausted CO_2 are eliminated. Instead, the CO_2 product is isolated and available for sequestration, or bottling for industrial use, with remaining levels recycled back into the closed system as a combustion diluent. Running this described system at supercritical conditions can further cut costs and increase its efficiency as the combined oxy-methane, with higher density supercritical CO_2 diluent (sCO_2), requires less pumping power for the same power output, while running with high power output comparable with conventional cycles (see Refs. [2–7] for sCO_2 power cycles).

In a full-flow staged combustion cycle used in rocket engines, both oxidizer and fuel pre-burners burn fuel lean and rich, respectively, in which all oxidizer and fuel flow through. Entering the main chamber are fuel-rich and oxygen-rich exhaust gases with products consisting of CO_2 and H_2O. As main combustion occurs in the presence of CO_2, the chemical kinetic understanding of oxy-methane diluted with CO_2 becomes important to accurately account for reactivity, especially at elevated pressures. SpaceX is in the midst of producing and testing such an engine, which is slated to operate at an astonishing chamber pressure of 300 bar—something that has never been achieved. This is the third engine ever to be developed and operational using the full-flow staged combustion cycle [8]; future endeavors and design optimizations will benefit from higher fidelity chemical kinetic mechanisms accounting for this reactivity.

Although CH_4 combustion is well understood across a variety of conditions and fuel loadings, the addition of CO_2 adds additional complexity that has not been accounted for in chemical kinetic mechanisms, as none of the validation work has been done with CO_2 as a primary diluent [9]. Furthermore, the effects of high fuel loading and the associated ignition behavior with immense CO_2 dilution have not been investigated in detail. Studies of oxy-methane combustion with CO_2 dilution have been performed in previous literatures [10–17], though largely at intermediate to lower pressures [14,18,19] in a shock tube. For example, Hargis and Peterson have investigated oxy-fuel combustion within a high-pressure shock tube at pressures from 1 to 10 atm and 1450 to 1900 K; it was observed that increasing the level of CO_2 led to increased bifurcation. Despite the presence of significant reflected-shock bifurcation in mixtures containing high levels of CO_2, the resulting ignition delay times were commensurate with calculated temperature and pressure behind reflected shock waves [20]. Other studies of oxy-methane mixtures include different levels of CO_2 dilution, but with a final conclusion finding that as the amount of CO_2 is increased, there is an insignificant, gradual increase in the ignition delay time [14,21,22], though as Hargis and Peterson [20] explain, this becomes more apparent at higher pressures. In an effort to extend the understanding of highly CO_2 dilute mixtures with high fuel loading, steps here are being made first at a moderate pressure with future work aimed at elevated pressures near 100 atm.

In the current work, a highly CO_2-diluted oxy-methane mixture was explored at pressures near 16 ± 2 atm and temperatures from 1044 to 1356 K. This mixture consisted of 16.67% CH_4, 33.33% O_2, and 50% CO_2. The CO_2 dilution was kept at a constant mole fraction of 0.5 in these experiments. The ignition delay times from these experiments were then compared with those of an oxy-methane mixture utilizing N_2 as a diluent consisting of 16.67% CH_4, 33.33% O_2, and 50% N_2. All gathered data were also compared with predictions by kinetic mechanisms, GRI Mech 3.0 [9] and ARAMCO 2.0 [23]. To the best of our knowledge, this study presents new insights into oxy-methane ignition with high levels of CO_2 dilution and high fuel loading.

Experimental Method

All experiments were performed in the high-purity, double-diaphragm shock tube facility located at the University of Central Florida in Orlando, Florida (see Refs. [11,18,24–31]). This shock tube has an internal diameter of 14.17 cm. Both sections were separated by a polycarbonate, scored diaphragm. In some cases, a stacked, double-diaphragm arrangement was used to achieve desired experimental conditions.

Before each experiment, both driver and driven sections were vacuumed down with Agilent DS102 rotary vane pumps to a rough level. The driven side was then further vacuumed down with an Agilent V301 turbomolecular pump; experiments were only proceeded with upon reaching a sufficient vacuum level on the order of 10^{-5} Torr or lower. Vacuum pressure was monitored with a convection and ion gauge from Kurt J. Lesker (KJL275804LL and KJLC354401YF, respectively).

The velocity of the incident shock wave was measured using five time-of-arrival pressure transducers (PCB 113B26) spaced at the last 1.4 m of the driven section (Fig. 1), which were attached to four timer-counters (Agilent 53220A, 0.1 ns resolution); this calculated velocity was then extrapolated to the end wall (EW) section. With velocity known, the temperature (T5) and pressure (P5) behind the reflected shock wave were then calculated using the 1-D ideal shock relations. For all experiments, attenuation of the incident shock wave was found to be less than 2%/m.

Mixtures were manometrically made using high purity gases from Praxair. Once the mixture was made, it was left to mix in a 33-L stainless steel mixing tank fitted with a magnetically driven stirrer. One Baratron (MKS 628D) was used to measure partial pressure during mixture preparation, which has an accuracy of ±0.5%.

The pressure behind the reflected shock wave was measured using sidewall-mounted Kistler 603B1 and PCB 113B26 pressure transducers located approximately 2 cm from the end wall. At the same location, emissions were measured with a New Focus UV photoreceiver (Model 2032) fitted with a 310 ± 10 nm filter supplied by Edmund Optics (Stock #67-752) targeting the excited radical OH*. A CO_2 gas laser (Access Laser L4GS) was aligned through the shock tube to aid in defining time-zero, via schlieren spikes; this will be discussed further in the sections "Nonidealities of the System" and "Results". Figure 2 shows the locations of these diagnostics.

Nonidealities of the System

Since all mixtures consisted of a diatomic (N_2) or polyatomic (CO_2) diluent, bifurcation was observed in all experiments.

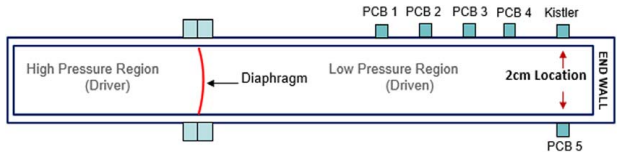

Fig. 1 Schematic of the shock tube facility indicating positions of pressure transducers and test section location

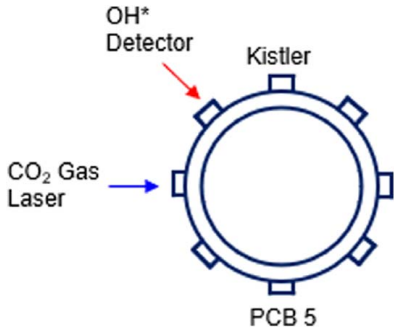

Fig. 2 Schematic showing circumferential positions of various diagnostics used (note this is in plane at the 2-cm location)

In these cases, a boundary layer forms lacking the necessary momentum (energy-deficient) to pass through the normal reflected shock wave and greatly interacts when compared to a monatomic bath gas like He or Ar. This interaction is more pronounced likely due to the increased molecular degrees-of-freedom. From Herman [32], it was shown that the relation between total pressure in the boundary layer and reflected shock wave determines the presence of bifurcation; through theory it was revealed that total pressure in the boundary layer is a function of incident shock Mach number and specific heat ratio of the test gas. This phenomenon results in two oblique shock waves in the boundary layer near the inside wall of the shock tube in the reflected shock front. As the flow passes through the second oblique shock wave, the velocity in this region parallel to the tube axis is nonzero while the velocity through the normal portion is stagnate, which induces a vortex sheet. Bifurcation can have multiple effects on the system, including a highly nonuniform velocity field, induced vorticity, and turbulence aiding in other nonuniformities and inhomogeneities [33–35]. The fluid flow issues imposed by bifurcation immensely affect pressure measurements as well, resulting in observed fluctuations or oscillations that increase with increasing amounts of CO_2, which ultimately add greater uncertainty [20]. Typically, end wall located diagnostics (pressure/emission) are preferred to understand ignition of non-dilute fuel mixtures primarily due to the tendency of sidewall-mounted diagnostics to observe earlier ignition delay times [36]. These earlier times are a result of a misinterpretation of time-zero due to bifurcation. Further explanation of our definition for time-zero will be discussed.

To elaborate on consequential nonuniformities that are presented in bifurcating systems, previous numerical work of Lamnaouer [37] revealed temperature and pressure gradients behind reflected shock waves, as well as hotspots in the wall jet after the passage of the bifurcation. In addition, Yamashita et al. [34] provide support for localized hotspots in bifurcated flows, and with the recent work of Lipkowicz et al. [35], it was shown that various gas dynamic and fluid dynamic structures occurred at a distance from the end wall supporting these localized nonuniformities due to the bifurcated shock. All of these features foster inhomogeneous (mild) ignition events, which start off as randomized hotspots.

Given that current mixtures explored had a very high fuel loading, this alone can ultimately lead to inhomogeneous (mild) ignition and deviation from ideal shock tube assumptions, as was discussed in previous literatures [38–41], among others. This phenomenon typically starts off as early energy/heat release from localized hotspots in a deflagrative manner, followed by a large release of energy leading to detonation, or detonation-to-deflagration transition (DDT) behavior [42]. In this current work, very strong detonations (blast wave) were formed in every experiment due to the immense energy release showing a distinct jump in pressure followed by oscillatory behavior of the blast wave. Because of this, a main definition of ignition delay time (IDT) can be defined from this pressure-jump.

Results and Discussion

Experiments were performed near 16 atm over a temperature range of 1044–1356 K with two main mixtures, consisting either of 50% CO_2 or N_2 as a diluent. Fuel concentration was kept at a high concentration of 16.67%. Table 1 shows a summary of all experiments performed. The table presents reflected temperatures and pressures, mixture composition, and various ignition definitions. The uncertainties in initial temperature and pressure behind reflected shock waves were ±10 K and 0.30 atm, respectively.

The ignition delay time has been defined considering two different overarching modes of auto-ignition that were observed in the current work. The definitions presented are adopted from the previous work of Fieweger et al. [42]. First, time-zero was defined by the reflected schlieren spike observed in the transmitted laser signal of the CO_2 gas laser aligned through the shock tube. This allowed for a lucid definition of time-zero over the pressure trace, as bifurcation presents difficulties in the interpretation of time-zero through the reflected pressure-rise measured with the sidewall-mounted pressure transducer. The first ignition delay time, τdefl, marks the beginning of the inhomogeneous early energy release, which initiates from very small localized hot spots or kernels. Quantifying this time was marked by the substantial rise in OH* signal. This phase of ignition proceeds as the hot spots develop, gradually consuming the mixture and leading to a detonation (blast wave). The immense pressure-rise associated with the secondary event was clearly evident and defined by the time of max dP5/dt, denoted as τDDT. These definitions are shown in Fig. 3.

The ignition definitions as described are compared to predictions from two chemical kinetic mechanisms, which will be presented in proceeding sections. A difficulty in assessing the performance of the mechanisms is the inevitable coupling of reflected shock wave bifurcation effects with early energy release (mild ignition). Were the latter not present, the former could then be accounted for with careful interpretation for valid comparison. Experiments exhibiting inhomogeneous ignition are not to be used in validating mechanisms, as 0-D homogeneous ideal shock tube behavior is not present; however, understanding the ignition behavior experimentally is paramount for future endeavors and can offer insight into the current system under these conditions. In addition, trends can be compared considering identical mixtures with N_2 or CO_2.

As was mentioned previously, due to the complex flows caused by bifurcation, pressure transducers are affected with the fluctuations of this flow. However, these diagnostics can offer potential resolve to the reflected shock wave–boundary layer interaction.

Table 1 Summary of current experiments

X_{CH_4}	X_{O_2}	X_{CO_2}	X_{N_2}	T_5 (K)	P_5 (atm)	τ_{defl} (ms)	τ_{DDT} (ms)
0.1667	0.3333	0.5	0.0	1097	15.76	1.080	1.358
				1162	15.38	0.747	1.090
				1314	14.64	0.310	0.589
				1197	15.35	0.435	0.904
				1289	14.05	0.294	0.614
				1356	14.55	0.267	0.367
				1091	16.87	0.946	1.024
				1073	16.61	0.594	1.083
				1045	17.46	1.018	1.776
0.1667	0.3333	0.0	0.5	1126	14.03	0.220	0.889
				1107	14.89	0.489	1.153
				1044	15.40	0.338	1.087

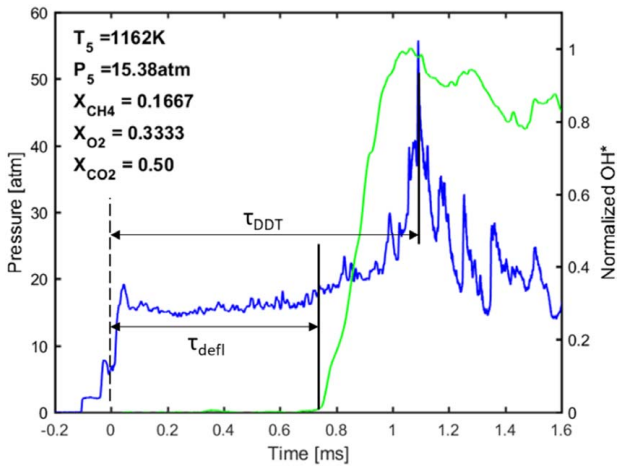

Fig. 3 Typical experimental pressure and emission traces with labeled definitions of ignition for the 50% CO_2-diluted mixture

Since a main definition of ignition was based on these pressure measurements, oscillations in the signal added uncertainty in the pressure rise, and thus added uncertainty in determining the time of the blast wave (τDDT). A region of ignition representative of this uncertainty is shown in Fig. 4. Because of this, the time of DDT was interpreted on a case-by-case basis, as was done previously by Hargis and Peterson [20]. The associated uncertainty in τDDT was larger than any uncertainty in T5 or P5, with the most impacted experiment revealing a 48% uncertainty in this ignition definition.

Understanding the implications of fluid fluctuations from bifurcation is clearly deduced from the pressure trace; another result of reflected shock–boundary layer in highly CO_2-diluted systems is an associated pressure rise (dP5/dt). From this pressure rise, a temperature rise can be modeled assuming an isentropic process [43]. The pressure rise as discussed previously [44] can be an order of magnitude higher in mixtures with CO_2 when compared to that in mixtures of Ar. Though in this current study, this is not easily distinguishable, as the pressure rise is also a result of ignition due to the large energy release of non-dilute mixtures (high fuel loading). Estimations were carried out carefully assessing the pressure traces on a case-by-case basis, keeping in mind the uncertainty due to pressure fluctuations and utilizing the definition of τdefl to narrow the region of interest. It should be noted that these estimations are not recommended, as there is an inherent coupled effect as discussed previously. For the 50% CO_2-diluted mixtures, dP5/dt was found to be between 2.4 and 32.5%/ms, and for the 50% N_2 mixtures 11.2–49.2%/ms, resulting in over 16 K and 34 K temperature increases, respectively. Again, the interpretation of this is clouded with the coupled effects; nevertheless, we determined dP5/dt was not directly correlated with temperature, and mixtures with N_2 had a larger dP5/dt. This agrees with discussion in the study by Hargis and Petersen [44]. Further investigation of 50% dilution at these conditions should be properly carried out with the use of nonreactive mixtures, whereby the associated effects of bifurcation on pressure and temperature rise can be characterized. This will be the focus of the ongoing work. To better understand the ignition data gathered, the pressure traces of the four PCBs spaced away from the test section (2 cm from end wall) were examined. This revealed interestingly that the arrival of the blast wave, in more cases than not, was captured at the PCB4 location first, followed by PCB5, PCB3, and so on. An example of this behavior for a given test can be seen in Fig. 5. Experiments where this was observed are considered as inhomogeneous. All of the N_2-diluted oxy-methane experiments exhibited this behavior, while the CO_2-diluted mixtures showed a correlation between temperature and ignition type (homogeneous/inhomogeneous). With all recorded PCB traces showing the arrival of the detonation, and known locations of each port, detonation traces were mapped,

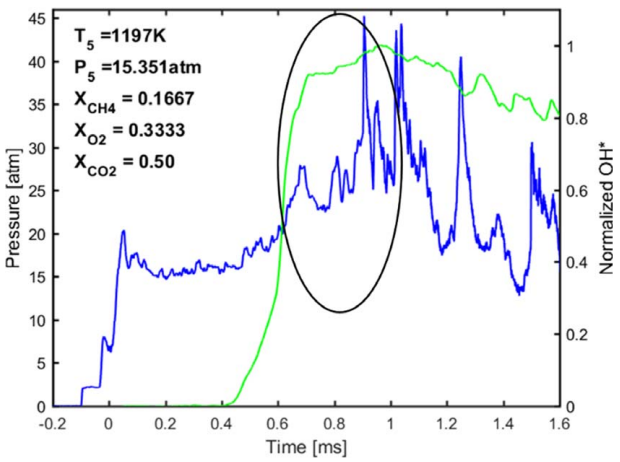

Fig. 4 Pressure and emission traces for the 50% CO_2-diluted mixture shown with a circled region of ignition

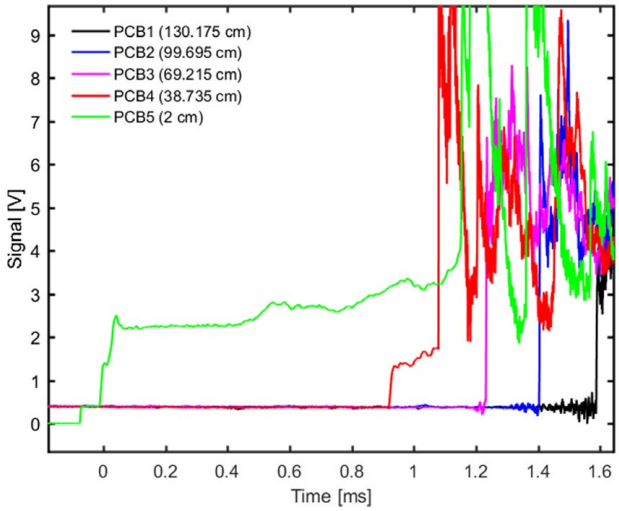

Fig. 5 Pressure traces measured via PCBs showing arrival of detonation with noted location from the end wall

which enabled the calculation of blast wave velocities for each experiment. Homogeneous (strong) ignition cases exhibited the onset of detonation in the test section as expected, which propagated back down the driver section away from the end wall. Such events with the associated detonation traces are shown in Fig. 6(*a*). The strong ignition cases show a clear linear first-order relationship that indicates a nearly constant blast wave velocity propagating away from the end wall.

Inhomogeneous events (as in Fig. 6(*b*)) did not show such a trend, but were rather divergent. From this, we inferred that the initiation of the detonation occurred somewhere between PCB4 and PCB5; if the centroid of a particular event were to propagate with a constant axial velocity away and toward the end wall, then we could further infer that the blast wave began closer to PCB4. With these reasonable assumptions, deduced from observation of the various pressure traces, a precise location can be calculated upon where the preignition event began. The validity of this assumption was not to be used if large acceleration toward the end wall was observed, deviating from a more or less similar constant velocity propagation in either direction. This was the case for one experiment at 1045 K and 17.46 atm. Table 2 lists the calculated blast wave velocities and locations of both homogeneous and inhomogeneous events for each experiment at reflected shock conditions. It should be noted that these reflected shock conditions are not representative of the detonation itself. Most calculated velocities are in good agreement of about 60–80% of the simulated CJ-Detonation velocities using a chemical equilibrium solver. It is evident that at temperatures below about 1197 K the CO_2-diluted mixtures enter a regime of inhomogeneous ignition behavior. Considering the N_2-diluted mixtures, higher temperature experiments would have been beneficial for a comprehensive comparison with CO_2-diluted mixtures; however, at temperatures higher than 1126 K the large energy release was so intense that detonation occurred upon the reflected shock wave, yielding no test time.

From Lipkowisz et al. [35], it was discussed through numerical methods employing large eddy simulation (LES) that bifurcation in a system can lead to the formation of a fluid-formed converging-diverging nozzle adjacent to the boundary layer inside the shock tube. As explained, subsonic fluid passes through the small initial bifurcated structure, which accelerates through the convergent part and subsequently becomes supersonic while compressed through the divergent part. At this point, the bifurcated structure grows further, promoting supersonic fluid to accelerate more so. The authors are insisting that because the bifurcated structure continues to grow past the choke point, the reflected shock conditions will be changed. Axial temperature and pressure profiles output

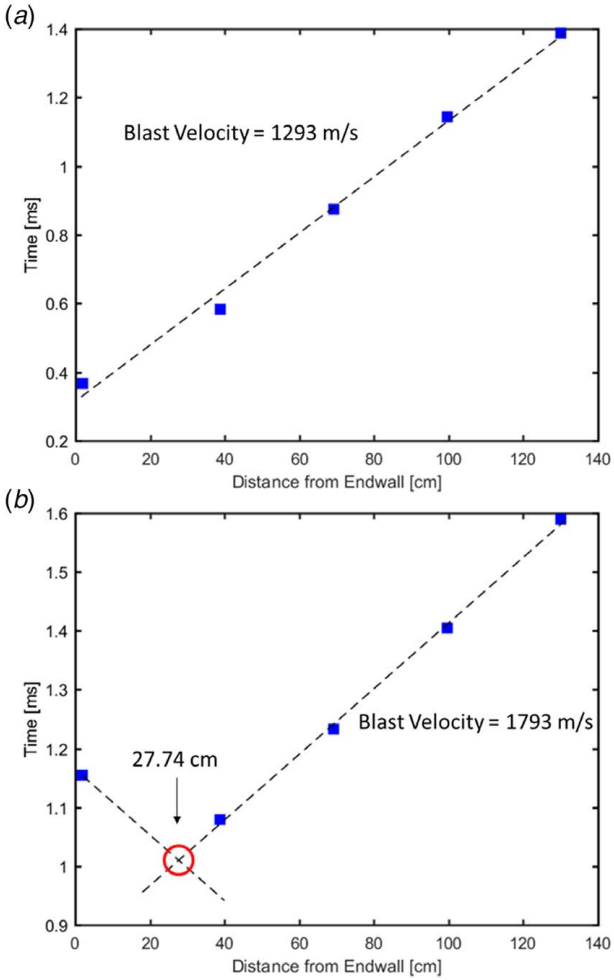

Fig. 6 Experimental detonation maps for (*a*) a homogeneous ignition event from the CO_2-diluted mixture and (*b*) an inhomogeneous ignition event from the N_2-diluted mixture; blast location is marked by an open red circle. Blast velocities and location are shown.

from their simulations revealed peaks behind reflected shock waves that were significantly higher than T5 and P5. Most interestingly, this showed that temperature increases with end wall distance, reaching a maximum around 60 mm (dependent upon the shock tube design), while pressure decreased monotonically. Their observations are in agreement with a previous numerical study of Weber et al. [45].

Table 2 Calculated blast wave velocities and initiation locations with corresponding defined ignition types

T_5 (K)	P_5 (atm)	Blast vel (m/s)	Blast location from EW (cm)	Preignition?
1097	15.76	872.2	31.98	Yes
1162	15.38	1213	23.93	Yes
1314	14.64	1753	Test section	No
1197	15.35	2341	Test section	No
1289	14.05	1641	Test section	No
1356	14.55	1293	Test section	No
1091	16.87	1180	22.10	Yes
1073	16.61	1378	26.04	Yes
1045	17.46	1192	NA	Yes
1126	14.03	1628	24.56	Yes
1107	14.89	1793	27.74	Yes
1044	15.40	1625	31.43	Yes

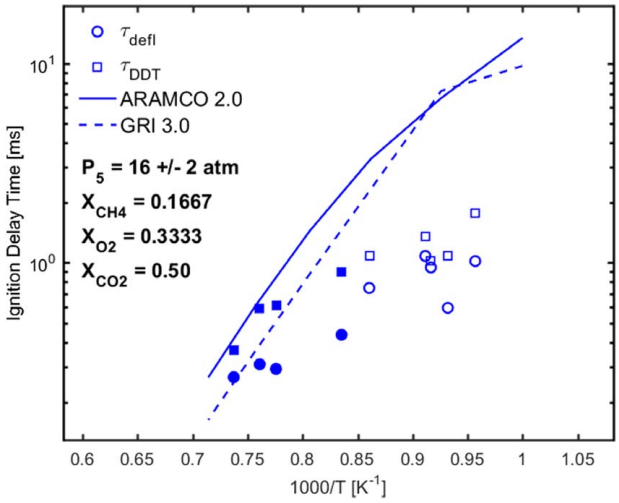

Fig. 7 Experimental definitions of ignition delay times compared to model predictions using chemkin-pro of the CO_2-diluted mixture. Homogeneous events are indicated with filled in markers.

The distance at which maximum temperature occurred was consistent across all simulations, which correlated well with the initiation of ignition. This supports the mild ignition observations of the current study, and the rather consistent location of initiation. The effects of shock wave attenuation should also be noted, as this will impact the strength of oblique shock waves and subsequent growth of the bifurcated structure in the divergent section. Typically, the arrival of a detonation is a good indication for the chemical ignition delay time, with the onset of secondary explosions representing a more or less homogeneous event [42]. While this may be true for mixed ignition regimes (transition from mild to strong ignition), this is not the case in the current work. An explanation for this may stem from the inherent high fuel loading, coupled with higher temperatures farther away from the end wall due to exacerbated bifurcation from CO_2/N_2, ultimately giving rise to an immense energy release tripping the formation of a detonation.

A comparison of experimental definitions of ignition to predictions of two chemical kinetic mechanisms in the literature is presented in Figs. 7–9. Simulations were performed using

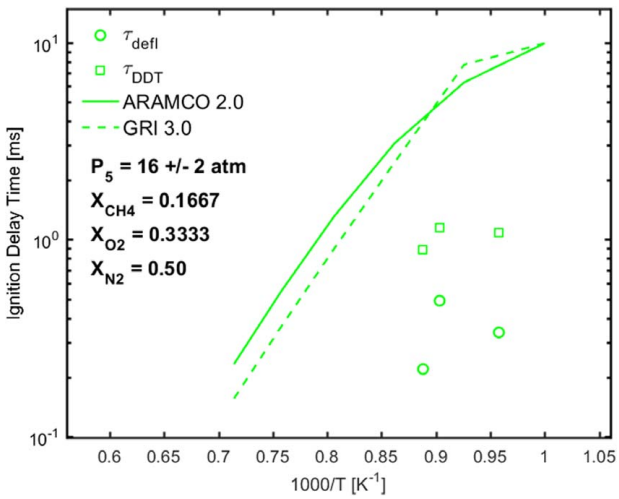

Fig. 8 Experimental definitions of ignition delay times compared to model predictions using chemkin-pro of the N_2-diluted mixture. Inhomogeneous events are indicated with open circles and squares.

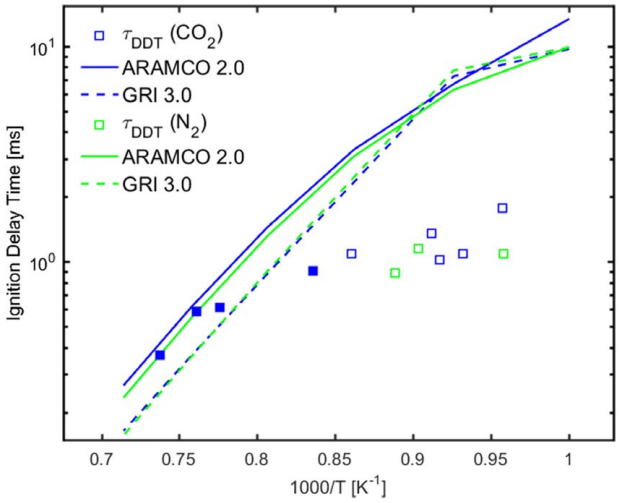

Fig. 9 Experimental ignition delay times based on immense pressure rise associated with detonation arrival compared to model predictions using chemkin-pro. Both $CH_4/O_2/CO_2$ and $CH_4/O_2/N_2$ mixture data are presented.

Chemkin-Pro [46] with a 0-D homogeneous bath reactor assuming the constant-U, V model, which is typically done for shock tube chemical kinetic simulations. As was alluded to previously, since inhomogeneous or preignition was observed in nearly all experiments, comparing such model predictions to data cannot be used in the validation of any chemical kinetic mechanism, though these comparisons can reveal many other interesting perspectives on inhomogeneous systems. In Fig. 7, the data from the CO_2-diluted mixture are plotted with model predictions from ARAMCO and GRI mechanisms. The filled in plot markers indicate experiments where homogeneous (strong) ignition was observed, having occurred as expected in the test section approximately 2 cm from the end wall. All of these strong ignition cases are present in the highest temperatures within the spread, which shows generally good agreement with model predictions: however, as temperature decreases all experiments deviate from predictions, revealing quicker IDTs. Good agreement has been shown previously at higher temperatures from low to elevated pressures. Interestingly, data from Shao et al. [10] show that at lower temperatures at a pressure near 250 atm, in comparison with predictions from ARAMCO, are in very good agreement, even with fairly high fuel loading of 3.91% and 7.5% CH_4. These data are indicative of strong ignition cases where preignition did not seem to be an overarching issue.

Comparing the various definitions of ignition, it is clearly shown that τDDT shows a definite trend (Fig. 9), while τdefl has no concrete relationship. The deflagrative ignition time is a measure of the initial stages of early energy release that has an incredible variance with each experiment. The randomized nature underscores nonuniformities that are present and the sensitivity of the system to them. Some of these nonuniformities include boundary layer, turbulence, bifurcation, surface effects, among others which cause unwanted perturbations [47,48].

Figure 8 shows experimental data and model predictions from the N_2-diluted mixture revealing all inhomogeneous cases. Mixtures containing N_2 as a bath gas do not absorb as much released energy from ignition events when compared to CO_2 and therefore promotes faster ignition. In addition, these mixtures were inherently more prone to ignite, and detonate within the incident conditions, or upon the reflected incident normal shock wave. These experiments gave no test time and were not used in this study.

Considering current conditions studied, the majority of the data acquired are not recommended in efforts to further refine chemical kinetic mechanisms. That being said, the insights into various ignition behavior have been analyzed, defined, and quantified, which revealed additional perspective on this combustion system. This included the necessary care that must be taken when assessing and defining various ignition behavior for non-dilute mixtures and ways to better analyze this through detonation maps. The onset of blast waves was also located, and most were found to be at great distances from the end wall commensurate with findings from previous literature discussed. In addition, the nonuniform effects of bifurcation due to CO_2 were investigated, which included pressure fluctuation and rise behind the reflected shock, and the consequences on experimental determination of IDT. The current level of high fuel loading presents additional data that can be useful; however, this should be limited only to higher temperatures.

Conclusion

Ignition delay time experiments have been recorded within the pressure range of 16 ± 2 atm for oxy-methane combustion diluted with carbon dioxide and nitrogen in a shock tube. The experiments were performed between 1044 K and 1356 K with a constant 50% CO_2 or N_2 dilution. Both OH* and pressure time traces were utilized to determine ignition delay times with two main modes of ignition defined: deflagration and detonation ignition delay time, τdefl and τDDT, respectively. Ignition behavior inside the shock tube was examined via the time of arrival PCB pressure transducers. These pressure traces enabled creation of detonation maps from which blast wave velocities were calculated. In addition to this, with reasonable assumptions, the precise onset of the detonations was inferred and quantified. From this each experiment was able to identify with a particular ignition regime, indicative of either strong or mild ignition. Most experiments showed mild (inhomogeneous) ignition. Comparisons with ARAMCO and GRI mechanisms revealed validity (and good agreement) for higher temperatures, but significant deviation as the temperature decreased. The nature of inhomogeneous ignition is such that comparisons with predictions from chemical kinetic mechanisms are not valid, though various trends were qualitatively deduced.

There is still much to kinetically investigate and validate regarding oxy-methane combustion systems in the presence of high CO_2 dilution. Future efforts will investigate the kinetics at higher temperatures, with an extension to elevated pressures, including higher fuel loadings as well. The latter of which may be confined to lower temperatures that are conducive to inhomogeneous ignition behavior, in addition to complexities from a bifurcating system. Including more investigations on non-dilute systems is more representative of real fuel/air mixtures, though increased energy release is likely to impact conditions behind reflected shock waves. This makes it difficult to distinguish nonideal effects due to added CO_2, as energy release and nonideal effects are blended. As mentioned earlier, nonreacting mixtures at the desired conditions will be necessary to properly characterize boundary layer effects. Additionally, radical formation throughout the test time and ignition process will be investigated to aid in the further refinement of kinetic mechanisms with high levels of CO_2 dilution.

Acknowledgment

This report was prepared as an account of work sponsored by an agency of the United States Government. Neither the United States Government nor any agency thereof, nor any of their employees, makes any warranty, express or implied, or assumes any legal liability or responsibility for the accuracy, completeness, or usefulness of any information, apparatus, product, or process disclosed, or represents that its use would not infringe privately owned rights. Reference herein to any specific commercial product, process, or service by trade name, trademark, manufacturer, or otherwise does not necessarily constitute or imply its endorsement, recommendation, or favoring by the United States Government or any agency thereof. The views and opinions of authors expressed herein do not necessarily state or reflect those of the United States Government or any agency thereof.

Funding Data

- National Science Foundation (Grant No. OISE 1460045; Funder ID: 10.13039/501100008982).
- U.S. Department of Energy (Grant Nos. DE-FE0025260 and DE-EE0007982; Funder ID: 10.13039/100000015).

References

[1] Brooks, K. P., Hu, J., Zhu, H., and Kee, R. J., 2007, "Methanation of Carbon Dioxide by Hydrogen Reduction Using the Sabatier Process in Microchannel Reactors," Chem. Eng. Sci., **62**(4), pp. 1161–1170.
[2] Vesely, L., Manikantachari, K. R. V., Vasu, S., Kapat, J., Dostal, V., and Martin, S., 2018, "Effect of Impurities on Compressor and Cooler in Supercritical CO2 Cycles," ASME J. Energy Resour. Technol., **141**(1), p. 012003.
[3] Khadse, A., Blanchette, L., Kapat, J., Vasu, S., Hossain, J., and Donazzolo, A., 2018, "Optimization of Supercritical CO2 Brayton Cycle for Simple Cycle Gas Turbines Exhaust Heat Recovery Using Genetic Algorithm," ASME J. Energy Resour. Technol., **140**(7), p. 071601.
[4] Black, J., Straub, D., Robey, E., Yip, J., Ramesh, S., Roy, A., and Searle, M., 2020, "Measurement of Convective Heat Transfer Coefficients With Supercritical CO2 Using the Wilson-Plot Technique," ASME J. Energy Resour. Technol., **142**(7), p. 070901.
[5] Deshmukh, A., and Kapat, J., 2020, "Pinch Point Analysis of Air Cooler in Supercritical Carbon Dioxide Brayton Cycle Operating Over Ambient Temperature Range," ASME J. Energy Resour. Technol., **142**(5).
[6] Fang, L., Li, Y., Yang, X., and Yang, Z., 2019, "Analyses of Thermal Performance of Solar Power Tower Station Based on a Supercritical CO2 Brayton Cycle," ASME J. Energy Resour. Technol., **142**(3), p. 031301.
[7] Bai, Z., Zhang, G., Yang, Y., and Wang, Z., 2019, "Design Performance Simulation of a Supercritical CO2 Cycle Coupling With a Steam Cycle for Gas Turbine Waste Heat Recovery," ASME J. Energy Resour. Technol., **141**(10), p. 102001.
[8] Livingjw, February 2019, "Raptor Engine Unoffical Combustion Scheme," Raptor Engine Unofficial Combustion Scheme.svg, ed., Creative Commons Attribution-ShareAlike 4.0 International. http://forum.nasaspaceflight.com/index.php?topic=47383.20
[9] Smith, G. P., Golden, D. M., Frenklach, M., Moriarty, N. W., Eiteneer, B., Goldenberg, M., Bowman, C. T., Hanson, R. K., Song, S., and Gardiner, W. C., 1999, *GRI-Mech 3.0*, Gas Research Institute, Chicago, IL.
[10] Shao, J., Choudhary, R., Davidson, D. F., Hanson, R. K., Barak, S., and Vasu, S., 2019, "Ignition Delay Times of Methane and Hydrogen Highly Diluted in Carbon Dioxide at High Pressures up to 300 atm," Proc. Combust. Inst., **37**(4), pp. 4555–4562.
[11] Barak, S., Pryor, O., Ninnemann, E., Neupane, S., Vasu, S., Lu, X., and Forrest, B., 2020, "Ignition Delay Times of Oxy-Syngas and Oxy-Methane in Supercritical CO2 Mixtures for Direct-Fired Cycles," ASME J. Eng. Gas Turbines Power, **142**(2), p. 021014.
[12] Barak, S., Pryor, O., Ninnemann, E., Neupane, S., Lu, X., Forrest, B., and Vasu, S., "Ignition Delay Times of Syngas and Methane in sCO2 Diluted Mixtures for Direct-Fired Cycles," Proceedings of ASME Turbo Expo 2019: Turbomachinery Technical Conference and Exposition, Phoenix, AZ, June 17–21, p. V009T38A001.
[13] Manikantachari, K. R. V., Vesely, L., Martin, S., Bobren-Diaz, J. O., and Vasu, S., 2018, "Reduced Chemical Kinetic Mechanisms for Oxy/Methane Supercritical CO2 Combustor Simulations," ASME J. Energy Resour. Technol., **140**(9), p. 092202.
[14] Pryor, O., Barak, S., Lopez, J., Ninnemann, E., Koroglu, B., Nash, L., and Vasu, S., 2017, "High Pressure Shock Tube Ignition Delay Time Measurements During Oxy-Methane Combustion With High Levels of CO2 Dilution," ASME J. Energy Resour. Technol., **139**(4), p. 042208.
[15] Almansour, B., Thompson, L., Lopez, J., Barari, G., and Vasu, S. S., 2016, "Laser Ignition and Flame Speed Measurements in Oxy-Methane Mixtures Diluted With CO2," ASME J. Energy Resour. Technol., **138**(3), p. 032201.
[16] Wang, Z., Yelishala, S. C., Yu, G., Metghalchi, H., and Levendis, Y. A., 2019, "Effects of Carbon Dioxide on Laminar Burning Speed and Flame Instability of Methane/Air and Propane/Air Mixtures: A Literature Review," Energy Fuels, **33**(10), pp. 9403–9418.
[17] Yelishala, S. C., Wang, Z., Metghalchi, H., Levendis, Y. A., Kannaiyan, K., and Sadr, R., 2019, "Effect of Carbon Dioxide on the Laminar Burning Speed of Propane–Air Mixtures," ASME J. Energy Resour. Technol., **141**(8), p. 082205.
[18] Koroglu, B., Pryor, O. M., Lopez, J., Nash, L., and Vasu, S. S., 2016, "Shock Tube Ignition Delay Times and Methane Time-Histories Measurements During Excess CO2 Diluted Oxy-Methane Combustion," Combust. Flame, **164**, pp. 152–163.
[19] Pryor, O., Barak, S., Koroglu, B., Ninnemann, E., and Vasu, S. S., 2017, "Measurements and Interpretation of Shock Tube Ignition Delay Times in Highly CO2 Diluted Mixtures Using Multiple Diagnostics," Combust. Flame, **180**, pp. 63–76.
[20] Hargis, J. W., and Petersen, E. L., 2015, "Methane Ignition in a Shock Tube With High Levels of CO2 Dilution: Consideration of the Reflected-Shock Bifurcation," Energy Fuels, **29**(11), pp. 7712–7726.
[21] Shareh, F. B., Silcox, G., and Eddings, E. G., 2018, "Calculated Impacts of Diluents on Flame Temperature, Ignition Delay, and Flame Speed of Methane–Oxygen Mixtures at High Pressure and Low to Moderate Temperatures," Energy Fuels, **32**(3), pp. 3891–3899.
[22] Sabia, P., Lubrano Lavadera, M., Sorrentino, G., Giudicianni, P., Ragucci, R., and de Joannon, M., 2016, "H_2O and CO2 Dilution in MILD Combustion of Simple Hydrocarbons," Flow, Turbul. Combust., **96**(2), pp. 433–448.
[23] Li, Y., Zhou, C.-W., Somers, K. P., Zhang, K., and Curran, H. J., 2017, "The Oxidation of 2-Butene: A High Pressure Ignition Delay, Kinetic Modeling Study and Reactivity Comparison With Isobutene and 1-Butene," Proc. Combust. Inst., **36**(1), pp. 403–411.
[24] Loparo, Z. E., Ninnemann, E., Ru, Q., Vodopyanov, K. L., and Vasu, S. S., 2020, "Broadband Mid-Infrared Optical Parametric Oscillator for Dynamic High-Temperature Multi-Species Measurements in Reacting Systems," Opt. Lett., **45**(2), pp. 491–494.
[25] Barak, S., Rahman, R. K., Neupane, S., Ninnemann, E., Arafin, F., Laich, A., Terracciano, A. C., and Vasu, S. S., 2020, "Measuring the Effectiveness of High-Performance Co-Optima Biofuels on Suppressing Soot Formation at High Temperature," Proc. Natl. Acad. Sci. U. S. A., **117**(7), pp. 3451–3460.
[26] Ninnemann, E., Kim, G., Laich, A., Almansour, B., Terracciano, A. C., Park, S., Thurmond, K., Neupane, S., Wagnon, S., Pitz, W. J., and Vasu, S. S., 2019, "Co-optima Fuels Combustion: A Comprehensive Experimental Investigation of Prenol Isomers," Fuel, **254**, p. 115630.
[27] Loparo, Z. E., Muraviev, A. V., Figueiredo, P., Lyakh, A., Peale, R. E., Ahmed, K., and Vasu, S. S., 2018, "Shock Tube Demonstration of Acousto-Optically Modulated Quantum Cascade Laser as a Broadband, Time-Resolved Combustion Diagnostic," ASME J. Energy Resour. Technol., **140**(11), p. 112202.
[28] Barak, S., Ninnemann, E., Neupane, S., Barnes, F., Kapat, J., and Vasu, S., 2019, "High-Pressure Oxy-Syngas Ignition Delay Times With CO2 Dilution: Shock Tube Measurements and Comparison of the Performance of Kinetic Mechanisms," ASME J. Eng. Gas Turbines Power, **141**(2), p. 021011.
[29] Loparo, Z. E., Lopez, J. G., Neupane, S., Partridge, W. P., Vodopyanov, K., and Vasu, S. S., 2017, "Fuel-Rich n-Heptane Oxidation: A Shock Tube and Laser Absorption Study," Combust. Flame, **185**(Supplement C), pp. 220–233.
[30] Barari, G., Pryor, O., Koroglu, B., Lopez, J., Nash, L., Sarathy, S. M., and Vasu, S. S., 2017, "High Temperature Shock Tube Experiments and Kinetic Modeling Study of Diisopropyl Ketone Ignition and Pyrolysis," Combust. Flame, **177**, pp. 207–218.
[31] Koroglu, B., and Vasu, S. S., 2016, "Measurements of Propanal Ignition Delay Times and Species Time Histories Using Shock Tube and Laser Absorption," Int. J. Chem. Kinet., **48**(11), pp. 679–690.
[32] Herman, M., 1958, "The Interaction of a Reflected Shock Wave With the Boundary Layer in a Shock Tube," *Technical Report*, National Advisory Committee for Aeronautics, Ithaca, NY.
[33] Kleine, H., Lyakhov, V. N., Gvozdeva, L. G., and Grönig, H., Bifurcation of a Reflected Shock Wave in a Shock Tube," *Proc. Shock Waves*, K Takayama, ed., Springer, Berlin/Heidelberg, pp. 261–266.
[34] Yamashita, H., Kasahara, J., Sugiyama, Y., and Matsuo, A., 2012, "Visualization Study of Ignition Modes Behind Bifurcated-Reflected Shock Waves," Combust. Flame, **159**(9), pp. 2954–2966.
[35] Lipkowicz, J. T., Wlokas, I., and Kempf, A. M., 2018, "Analysis of Mild Ignition in a Shock Tube Using a Highly Resolved 3D-LES and High-Order Shock-Capturing Schemes," Shock Waves, **29**(6), pp. 511–521.
[36] Petersen, E. L., 2009, "Interpreting Endwall and Sidewall Measurements in Shock-Tube Ignition Studies," Combust. Sci. Technol., **181**(9), pp. 1123–1144.
[37] Lamnaouer, M., 2014, "A Conjugate Axisymmetric Model of a High-Pressure Shock-Tube Facility," Int. J. Numer. Methods Heat Fluid Flow, **24**(4), pp. 873–890.
[38] Figueroa-Labastida, M., Badra, J., Elbaz, A. M., and Farooq, A., 2018, "Shock Tube Studies of Ethanol Preignition," Combust. Flame, **198**, pp. 176–185.
[39] Chaos, M., and Dryer, F. L., 2010, "Chemical-kinetic Modeling of Ignition Delay: Considerations in Interpreting Shock Tube Data," Int. J. Chem. Kinet., **42**(3), pp. 143–150.
[40] Laich, A. R., Ninnemann, E., Neupane, S., Rahman, R., Barak, S., Pitz, W. J., Goldsborough, S. S., and Vasu, S. S., 2020, "High-Pressure Shock Tube Study of Ethanol Oxidation: Ignition Delay Time and CO Time-History Measurements," Combust. Flame, **212**, pp. 486–499.
[41] Mathieu, O., Pinzón, L. T., Atherley, T. M., Mulvihill, C. R., Schoel, I., and Petersen, E. L., 2019, "Experimental Study of Ethanol Oxidation Behind Reflected Shock Waves: Ignition Delay Time and H_2O Laser-Absorption Measurements," Combust. Flame, **208**, pp. 313–326.
[42] Fieweger, K., Blumenthal, R., and Adomeit, G., 1997, Self-ignition of S.I. engine model fuels: A shock tube investigation at high pressure.
[43] Petersen, E. L., and Hanson, R. K., 2001, "Nonideal Effects Behind Reflected Shock Waves in a High-Pressure Shock Tube," Shock Waves, **10**(6), pp. 405–420.
[44] Hargis, J. W., and Petersen, E. L., 2017, "Shock-Tube Boundary-Layer Effects on Reflected-Shock Conditions with and Without CO2," AIAA J., **55**(3), pp. 902–912.
[45] Weber, Y. S., Oran, E. S., Boris, J. P., and Anderson, J. D., 1995, "The Numerical Simulation of Shock Bifurcation Near the end Wall of a Shock Tube," Phys. Fluids, **7**(10), pp. 2475–2488.
[46] ANSYS, 2019, "Chemkin-Pro," San Diego, CA.
[47] Meyer, J. W., and Oppenheim, A. K., 1971, "On the Shock-Induced Ignition of Explosive Gases," Symp.Combust., **13**(1), pp. 1153–1164.
[48] Chaos, M., and Dryer, F. L., 2008, "Syngas Combustion Kinetics and Applications," Combust. Sci. Technol., **180**(6), pp. 1053–1096.